



Virginia Commonwealth University  
VCU Scholars Compass

Electrical and Computer Engineering Publications

Dept. of Electrical and Computer Engineering

2011

# Field-assisted emission in AlGaN/GaN heterostructure field-effect transistors using low-frequency noise technique

Cemil Kayis

*Virginia Commonwealth University, [ckayis@vcu.edu](mailto:ckayis@vcu.edu)*

C. Y. Zhu

*Virginia Commonwealth University*

Mo Wu

*Virginia Commonwealth University*

*See next page for additional authors*

Follow this and additional works at: [http://scholarscompass.vcu.edu/egre\\_pubs](http://scholarscompass.vcu.edu/egre_pubs)

 Part of the [Electrical and Computer Engineering Commons](#)

Kayis, C., Zhu, C. Y., & Wu, M., et al. Field-assisted emission in AlGaN/GaN heterostructure field-effect transistors using low-frequency noise technique. *Journal of Applied Physics*, 109, 084522 (2011). Copyright © 2011 American Institute of Physics.

Downloaded from

[http://scholarscompass.vcu.edu/egre\\_pubs/157](http://scholarscompass.vcu.edu/egre_pubs/157)

This Article is brought to you for free and open access by the Dept. of Electrical and Computer Engineering at VCU Scholars Compass. It has been accepted for inclusion in Electrical and Computer Engineering Publications by an authorized administrator of VCU Scholars Compass. For more information, please contact [libcompass@vcu.edu](mailto:libcompass@vcu.edu).

---

**Authors**

Cemil Kayis, C. Y. Zhu, Mo Wu, X. Li, Ümit Özgür, and Hadis Morkoç

## Field-assisted emission in AlGaN/GaN heterostructure field-effect transistors using low-frequency noise technique

Cemil Kayis,<sup>a)</sup> C. Y. Zhu, Mo Wu, X. Li, Ümit Özgür, and Hadis Morkoç

Department of Electrical and Computer Engineering, Virginia Commonwealth University, Richmond, Virginia, USA 23284-3072

(Received 19 January 2011; accepted 12 March 2011; published online 27 April 2011)

We utilized low-frequency noise measurements to probe electron capture and emission from the traps in AlGaN/GaN heterostructure field-effect transistors as a function of drain bias. The excess noise-spectra due to generation-recombination effect shifted higher in frequency with the elevated temperature from room temperature up to 446 K. These temperature dependent noise measurements were carried out for four different drain-bias values from 4 up to 16 V with 4 V increments. The shift of the excess-noise in frequency was also seen with increasing drain bias. The characteristic recharging times for the trapped electrons varied within the range of 26  $\mu$ s – 32 ms for the highest and lowest values of the drain voltage and temperature used in the experiment, respectively. The activation energies of the traps corresponding to the four different voltage values were extracted using temperature dependence by Arrhenius analysis. The trap energy at zero drain-bias was obtained as 0.71 eV by the extrapolation technique. This result suggests that the LFN is a very sensitive diagnostic tool to characterize trap states. © 2011 American Institute of Physics. [doi:10.1063/1.3576104]

### I. INTRODUCTION

GaN based heterostructure field effect transistors (HFETs) exhibit remarkable performance in high frequency and high power applications.<sup>1</sup> However, the presence of electronic traps in the device structure is still a major problem and limits its performance and reliability.<sup>2</sup> Several techniques, such as deep-level transient spectroscopy,<sup>3–6</sup> low-frequency transconductance dispersion,<sup>7,8</sup> pulsed current transient spectroscopy,<sup>9,10</sup> and photoionization spectroscopy<sup>11,12</sup> as well as the standard transient current-voltage and capacitance-voltage methods<sup>13</sup>, have been used to identify these traps, their spatial locations and the effects on the device performance. Analyses of these traps can be made assuaged some by bringing to bear new tools. For example, the pulsed current-transient spectroscopy technique is not sensitive to shallow traps if the buffer layer suffers from the deep traps, for which the transient current recovery is too long. Thus, it is beneficial to implement more sensitive and versatile measurement techniques to monitor and characterize the charge traps in the HFET structure.

Low-frequency noise (LFN) spectra,<sup>14,15</sup> particularly those originating from generation-recombination (GR) processes,<sup>16,17</sup> are beneficial for analyzing semiconductor quality for both interface and bulk properties owing to the fluctuations in the channel-current being affected by capturing and emission of the electrons.<sup>18,19</sup>

In this manuscript, we show that a specific LFN, measured with an integrated residual phase-noise setup, is able to detect the additive noise contribution to find the activation energy of a dominant GR-noise yielding defect(s) at various drain bias values. Using the activation energy values of the

traps extracted from the temperature- dependent measurements corresponding to each bias condition, we obtained the dominant trap energy level at zero applied drain bias.

### II. EXPERIMENTAL

We carried out the noise measurements using an Agilent E5505A test-set with a built-in phase detector (mixer) [Fig. 1]. Setting the input ports of the mixer 90 degrees out of phase, we measured the residual phase fluctuations of the HFETs at certain bias conditions. The single-sided-spur calibration technique was used to achieve the maximum sensitivity using an extra signal generator. The main difference between our technique and the baseband method<sup>17,20</sup> is simply the application of high-frequency carrier signal. We applied a 4 GHz signal

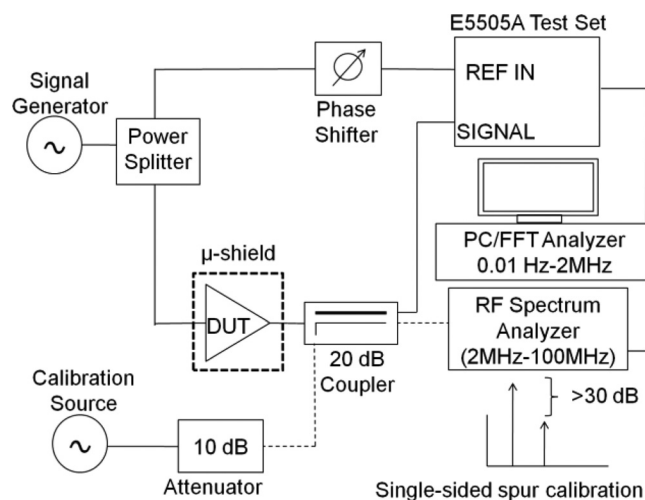


FIG. 1. Block diagram of the Agilent E5505 residual phase-noise measurement setup with the single-sided spur calibration technique.

<sup>a)</sup>Electronic mail: ckayis@vcu.edu.

with an input power of approximately 1 mW and monitored the single-sideband low-frequency response within a 100 MHz offset frequency. We noted the corner frequencies spanning up to 1 MHz using the residual phase-noise technique. The corner frequencies observed using baseband method were about two orders of magnitude lower than the ones observed using the phase-noise technique at identical bias conditions. This allowed us to observe the noise levels below the noise floor afforded by the baseband method.<sup>21</sup>

### III. HFET PARAMETERS AND DC RESULTS

The HFET structure was grown on sapphire by metalorganic chemical vapor deposition (MOCVD). A 2.5- $\mu\text{m}$ -thick undoped GaN buffer was deposited following a 250-nm-thick AlN initiation layer on sapphire. Next, a 20-nm-thick AlGaIn barrier layer was grown with 25% Al mole fraction. The Hall-effect measurements yielded a sheet carrier density  $n_s \approx 1.2 \times 10^{13} \text{ cm}^{-2}$  and the electron mobility  $\mu_e \approx 960 \text{ cm}^2/\text{Vs}$  at room temperature. The source and drain contacts were formed using a standard lift-off technique and a Ti/Al/Ni/Au (30/100/40/50 nm thick) alloyed stack. Mesa isolation was performed in a SAMCO inductively coupled plasma (ICP) system using a Cl-based chemistry. After opening windows to the source and drain pads via ICP etching for electrical access, the gate electrodes were deposited using standard lift-off procedure with Pt/Au (30/50 nm-thick) electrodes. Figure 2(a) and 2(b) show the schematic diagrams of the HFET structure with the metal contacts and the conduction band of the buffer and the barrier. The typical  $I_D$  vs  $V_{DS}$  family output curves for the HFETs is shown in Fig. 2(c). Figure 2(d) shows the transfer properties of the HFETs with a maximum transconductance of 230 mS/mm and a maximum drain current of 520 mA/mm at  $V_{GS} = 0$ . The devices exhibited  $1.0 \times 10^{-4} \text{ A/mm}$  gate leakage at  $V_{GS} = -8 \text{ V}$  and a pinch-off voltage of  $-2.9 \text{ V}$ .

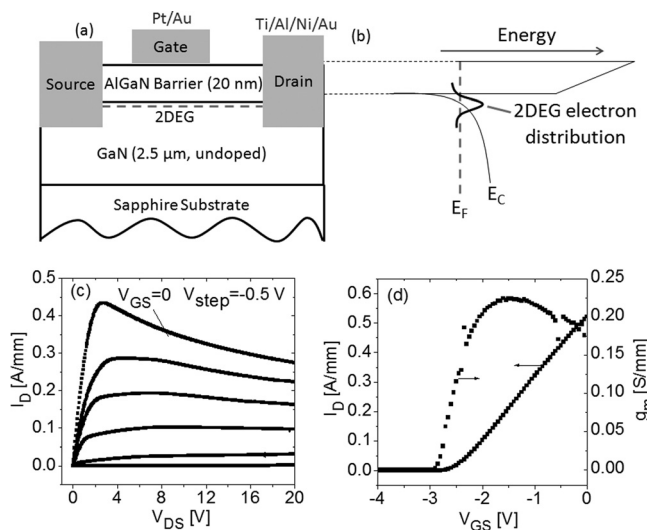


FIG. 2. (a) A top-down schematic diagram of the HFET layer structure with the ohmic and Schottky contacts. (b) The schematic conduction band diagram of the barrier and the buffer layers with the 2DEG distribution. (c) The  $I_D$  vs  $V_{DS}$  family of curves for the HFETs is seen with the increments of  $V_{GS}$  by  $-0.5 \text{ V}$ . (d) Transfer properties of the HFET devices.

### IV. LFN RESULTS AND DISCUSSIONS

The LFN measurements consistently manifested a broad additive-noise peak, which could be attributed to the generation-recombination (GR) noise arising from a definite trap level in the barrier or interface [Fig. 3]. This shows that the noise technique we used is sensitive to the trap-originated variations in the channel-noise spectra of the devices. The GR noise in an HFET originates from traps that randomly capture and emit electrons, thereby causing fluctuations in the number of electrons which carry current in the channel. The spectrum has two main components with one or more Lorentzians in addition to the  $1/f$  background. Thus, the noise-spectral-density (NSD) has the form of:<sup>17</sup>

$$\text{NSD} = S(f) = A/f^\gamma + \sum B_i \tau_i / (1 + (2\pi f)^2 \tau_i^2), \quad (1)$$

where  $\tau_i$  are the time constants associated with the above-mentioned transitions and  $\gamma$  is a parameter close to 1.  $A$  and  $B_i$  are the coefficients characterizing the crystal quality, trap concentration and number of electrons in the channel.

Trapping and detrapping are processes that have strong lattice-temperature dependence. Thus, an analysis of the position of the broad GR peaks in Fig. 3 with respect to temperature would allow us to extract the activation energy of the traps [Eq. (2)]. In order to achieve this, we acquired the data from room temperature up to 446 K, and noted the shift of the peaks toward higher frequencies with increasing temperature. We fit the peaks to a Lorentzian function according to Eq. (1) following the subtraction of the  $1/f^\gamma$  background from the GR spectra.<sup>16</sup> This allowed us to obtain the time constant for a certain temperature. Using the acquired trap characteristic times, the energy level of the traps can be found from the equation

$$\tau_T = \tau_0 \exp(E_T/kT), \quad (2)$$

where  $\tau_T$  is the trap time constant,  $E_T$  is the trap energy level below the conduction band,  $k$  is the Boltzmann constant. From the definition of Shockley-Read density,  $\tau_0$  is equal to  $(v_n \sigma_T N_c)^{-1}$ , where  $v_n \propto T^{1/2}$  is the average drift velocity of the electrons,  $\sigma_T$  is the capture cross section of the traps, and  $N_c \propto T^{3/2}$  is the density of states in the conduction band.<sup>17,22</sup>

The behavior of the additive GR contributed noise spectra at different drain bias conditions must be analyzed carefully to understand the physical mechanisms involved, which lead to spectrum shifts in the frequency axis. Hence, we can draw more conclusions related to the trap characteristics within the context of emission and capture processes. The activation energy  $E_A$  acquired from the Arrhenius analysis is the amount of energy to excite the localized electrons confined in the potential barrier of the traps to the conduction band at certain bias conditions. The deeper potential barrier results in larger activation energy with respect to the bottom of the conduction band and longer time constants according to Eq. (2). The trap potential barrier is skewed in the presence of an external electric field, which decreases the effective trap barrier in the opposite direction of the field vector for a hydrogenlike potential well. This case is important for

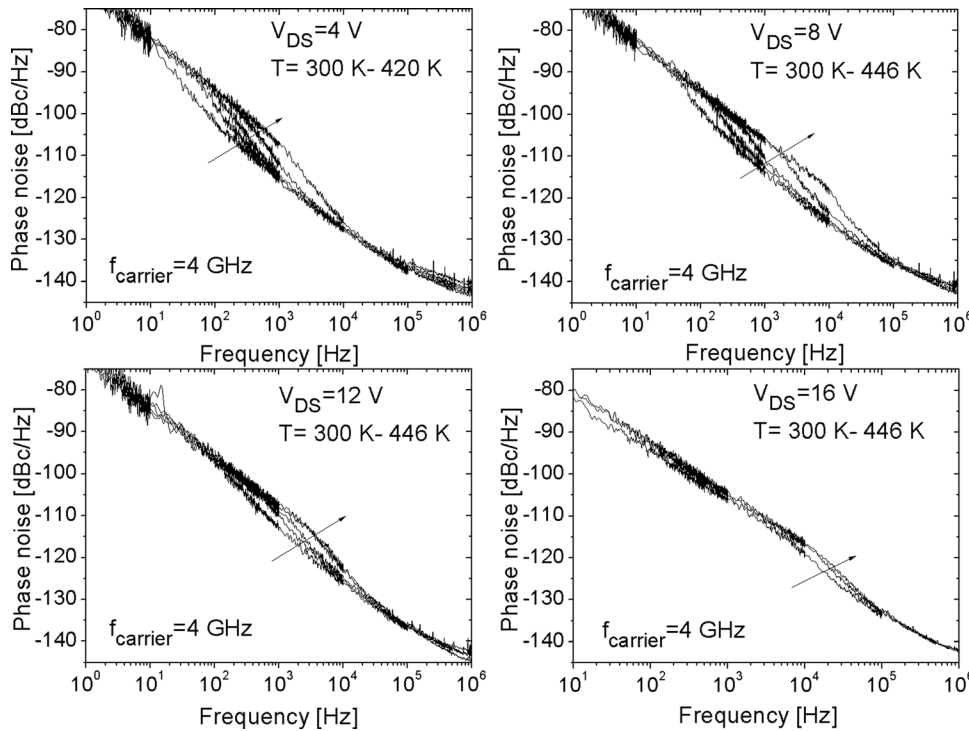


FIG. 3. Four sets of noise-spectral-density curves at  $V_{DS}$  values from 4 to 16 V within the indicated temperature ranges. The arrows show that the spectra shift higher in frequency with both increasing drain bias and temperature. The trap time constants vary from 0.1 to 32 ms for  $V_{DS} = 4$  V and from 30  $\mu$ s to 1.6 ms for  $V_{DS} = 12$  V. The broad Lorentzian feature of the spectra is predominantly due to the nonuniform electric field in the AlGaIn barrier region and variation in the trap barrier heights within the barrier or surface.

GaN based HFETs since there is a large external electric field in the barrier of the structure due to the applied drain-source bias. Naturally then we now turn our attention the effect of external electric field on the emission rates and on the lowering of the activation energy.

In the presence of a strong electric field, the effective trap potential barrier height can decrease remarkably, and consequently this increases the emission probability of the trapped electrons. This effect is known as the Frenkel – Poole effect and for a singly charged center the lowering of the potential barrier can be characterized as follows:<sup>1</sup>

$$\Delta\phi_{FP} = (q^3/\pi\epsilon_0\epsilon_r)^{1/2}F^{1/2}, \quad (3)$$

where  $q$  is the elementary electron charge,  $\epsilon_0\epsilon_r$  is the dielectric constant of the crystal, and  $F$  is the magnitude of the external electric field. Hence, we can rewrite Eq. (2) including the field dependency as

$$e(T, F) = AT^2 \exp[-(E_T - \Delta\phi_{FP})/kT], \quad (4)$$

where  $e(T, F)$  is the emission rate of the electrons and  $A$  is a field dependent preexponential factor. The field-dependent activation energy,  $E_A(F)$ , can be defined as the difference between the trap energy and the barrier lowering:

$$E_A(F) = E_A(0) - \Delta\phi_{FP} = E_T - (q^3/\pi\epsilon_0\epsilon_r)^{1/2}F^{1/2}, \quad (5)$$

where  $E_A(0) = E_T$  is the binding energy of the trapped electrons at  $F = 0$ . Knowing that the electric field is directly proportional to the applied voltage in continuous media, Eq. (5) gives

$$E_A(V_{DS}) = E_T - \beta V_{DS}^{1/2}, \quad (6)$$

where  $\beta$  is a constant.

In Fig. 3, we show the noise spectra for four different drain bias values. The noise spectra shift higher in frequency with the increasing temperature and drain-source bias as expected. The GR features monitored in the LFN spectra are broader and weaker than the data shown in Ref. 16 partly stemming from the traps experiencing the nonuniform electric field in the barrier layer, where the electric field is at its maximum value on the drain side of the gate.<sup>1</sup> This electric field gradient causes a variation in the amount of barrier lowering due to the Frenkel – Poole effect, which may broaden the additional noise peak. The Lorentzians can also be smeared out due to the inhomogeneous distribution of the barrier traps in the vertical direction.<sup>23</sup> Moreover, the weakening of the distinct GR spectrum can be attributed to the lower concentration of the traps with a certain time constant leading to the GR excess noise.

Assuming that the electron emission above room temperature dominated by the Frenkel – Poole mechanism in the AlGaIn barrier, we extracted the zero-field trap activation energy,  $E_T$ , using the following method.<sup>9,24</sup> First we measured the temperature dependent LFN for a device with 1  $\mu$ s gate length for four different drain-source bias conditions within the range of 4 – 16 V with 4 V increment to verify the validity of the FP model. All the measurements were performed at zero gate bias. Then we obtained the emission rates for each LFN spectrum from the additional Lorentzian characteristics of the spectra [Fig. 3].<sup>25</sup> The temperature and drain-bias dependent emission rates exhibited a wide range of values. The characteristic trap time constants calculated from these emission rates varied about three orders of magnitude within the range of 32 ms – 26  $\mu$ s for the temperature and bias values at (300 K, 4 V) and (446 K, 16 V), respectively.

We extracted the activation energy for each bias condition from temperature dependence using the Arrhenius analysis [Fig. 4]. The activation energy is simply the slope of the

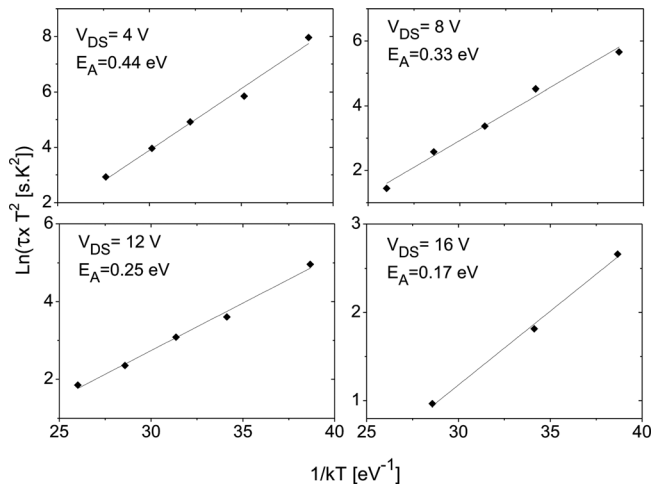


FIG. 4. The Arrhenius plots for all drain-source bias values for which the temperature-dependent low-frequency noise (LFN) measured. The plot at  $V_{DS} = 16$  V has only three data points since it is hard to extract the emission rates at the highest applied values of drain-bias and temperature combination.

$\ln(\tau x T^2)$  vs  $1/kT$  plot for a certain drain bias in units of eV [Eq. (2)]. The trap energies were found as 0.44, 0.33, 0.25, and 0.17 eV corresponding to the  $V_{DS} = (4, 8, 12, \text{ and } 16 \text{ V})$ , respectively. Figure 4 shows the Arrhenius plots at each bias condition and the corresponding activation energy values. The zero-bias binding energy is given as 0.71 eV in Fig. 5 by extrapolation, which is 0.27 eV lower than the activation energy at  $V_{DS} = 4$  V. It is obtained from the fit to the plot  $E_A(V_{DS})$  vs  $V_{DS}^{1/2}$  according to Eq. (6). This confirms that there is a substantial barrier lowering due to the external bias.

The dominant GR contribution to the noise spectra may arise spatially from the regions close by the channel. The additive feature of the GR noise has been investigated in detail in Ref. 15. According to the number fluctuation theory, a uniformly distributed trap concentration in the barrier layer causes the  $1/f$  noise in an HFET. The deviation from the  $1/f$  noise with a certain GR feature in the noise spectra obtained here implies that the trap concentration in the close vicinity of the channel is not uniform. This effect is important in

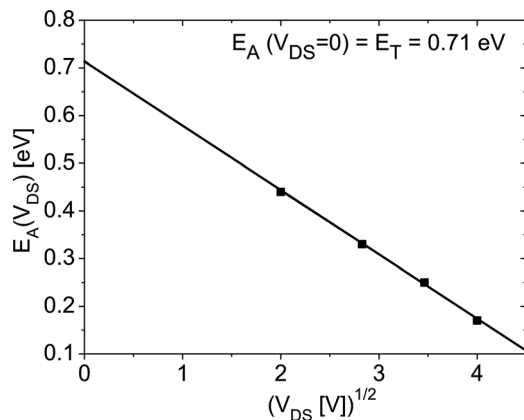


FIG. 5. Linear fit for the activation energy vs  $(V_{DS})^{1/2}$  plot [Eq. (6)]. Trap energy at zero bias can be extracted from the  $y$  intercept as 0.71 eV.

terms of the device reliability and performance which may cause generation of more traps under electrical stress.

## V. CONCLUSIONS

We employed low-frequency noise (LFN) measurements for AlGaIn/GaN HFETs and monitored the evolution of the channel-noise spectra as a function of drain-source bias in order to probe the trap characteristics. The activation energy at each bias point is obtained from the temperature dependence of the emission using Arrhenius analysis. The trap energy at zero-bias was extracted as 0.71 eV by extrapolation technique. The activation energy at a drain bias of 4 V was 0.44 eV. This validated that the barrier lowering due to the field-assisted emission (Frenkel – Poole effect) in the barrier layer is substantial. The nonuniform external field in the barrier layer causes the additive GR spectrum to have a broader feature. The dominant trap effect monitored here can arise from the regions in the vicinity of the channel. The results show that the LFN is a very sensitive and useful diagnostic tool to characterize the trap states in the AlGaIn/GaN HFETs.

## ACKNOWLEDGMENTS

VCU research is funded by a grant from the Air Force Office of Scientific Research under the guidance of Dr. K. Reinhardt. We thank Professor A. Matulino and Professor P. H. Handel for constructive discussions.

- <sup>1</sup>Hadis Morkoç, *Handbook on Nitride Materials and Devices* (Wiley, New York, 2009), Vol. 3, Chap. 3.
- <sup>2</sup>J. H. Leach and H. Morkoç, *Proc. IEEE* **98**, 1127–1139 (2010).
- <sup>3</sup>T. Okino, M. Ochiai, Y. Ohno, S. Kishimoto, K. Maezawa, and T. Mizutani, *IEEE Electron Device Lett.* **25**, 523–525 (2004).
- <sup>4</sup>A. V. Vertiatchikh, L. F. Eastman, W. J. Schaff, and T. Prunty, *IEEE Electronics Letters* **38**, 388 (2002).
- <sup>5</sup>A. Chini, M. Esposito, G. Meneghesso, and E. Zanoni, *Electron. Lett.* **45**, 426 (2009).
- <sup>6</sup>T. Mizutani, A. Kawano, S. Kishimoto, and K. Maezawa, *Phys. Status Solidi C* **4**, 1536 (2007).
- <sup>7</sup>A. Sozza, C. Dua, E. Morvan, M. A. diForte-Poisson, S. Delage, F. Rampazzo, A. Tazzoli, F. Danesin, G. Meneghesso, E. Zanoni, A. Curutchet, N. Malbert, N. Labat, B. Grimbert, and J.-C. De Jaeger, *Evidence of traps creation in GaN/AlGaIn/GaN HEMTs after a 3000 hour on-state and off-state hot-electron stress*, Proceedings Electron Devices Meeting, 2005, IEDM Technical Digest (IEEE International, Washington, D.C., 2005), p. 593.
- <sup>8</sup>W. Kruppa, S. C. Binari, and K. Doverspike, *IEEE Electron. Lett.* **31**, 1951 (1995).
- <sup>9</sup>O. Mitrofanov, and M. Manfra, *Superlattices Microstruct.* **34**, 33 (2003).
- <sup>10</sup>E. Kohn, I. Daumiller, M. Kunze, M. Neuburger, M. Seyboth, T. J. Jenkins, J. S. Sewell, J. Van Norstand, Y. Smorchkova, and U. K. Mishra, *IEEE Trans. Microwave Theory Techniques* **51**, 634–642 (2003).
- <sup>11</sup>P. B. Klein, S. C. Binari, J. A. Freitas, Jr., and A. E. Wickenden, *J. Appl. Phys.* **88**, 2843 (2000).
- <sup>12</sup>S. C. Binari, P. B. Klein, and T. E. Kazior, *Proc. IEEE* **90**, 1048–1058 (2002).
- <sup>13</sup>E. J. Miller, X. Z. Dang, H. H. Wieder, P. M. Asbeck, E. T. Yu, G. J. Sullivan, and J. M. Redwing, *J. Appl. Phys.* **87**, 8070 (2000).
- <sup>14</sup>L. K. J. Vandamme, *IEEE Trans. Electron Devices* **41**, 2176 (1994).
- <sup>15</sup>L. K. J. Vandamme and F. N. Hooge, *Physica B* **357**, 507 (2005).
- <sup>16</sup>C. Kayis, J. H. Leach, C. Y. Zhu, Mo Wu, X. Li, Ü. Özgür, H. Morkoç, X. Yang, V. Misra, and P. H. Handel, *IEEE Electron Device Lett.* **31**, 1041 (2010).
- <sup>17</sup>R. S. Duran and G. L. Larkins, Jr., C. M. Van Vliet, and H. Morkoç, *J. Appl. Phys.* **93**, 5337 (2003).
- <sup>18</sup>W. Shockley and W. T. Read, Jr., *Phys. Rev.* **87**, 835 (1952).

- <sup>19</sup>A. L. McWorther, *Semiconductor Surface Physics* (University of Pennsylvania Press, Philadelphia, 1957).
- <sup>20</sup>A. Balandin, S. Morozov, G. Wijeratne, S. J. Cai, R. Li, J. Li, K. L. Wang, C. R. Viswanathan, and Yu. Dubrovskii, *Appl. Phys. Lett.* **75**, 2064–2066 (1999).
- <sup>21</sup>C. Kayis, J. H. Leach, C. Y. Zhu, Mo Wu, X. Li, X. Yang, V. Misra, Peter H. Handel, Ü. Özgür, and H. Morkoç, “Measurements of generation-recombination effect by low-frequency phase-noise technique in AlGaIn/GaN MOSHFETs,” *Phys. Status Solidi C*, pp. 1–5 (2011)
- <sup>22</sup>P. Kordoš, R. Stoklas, D. Gregušová, and J. Novák, *Appl. Phys. Lett.* **94**, 223512 (2007).
- <sup>23</sup>C. M. Van Vliet, *J. Appl. Phys.* **93**, 6068 (2003).
- <sup>24</sup>H. Zhang, E. J. Miller, and E. T. Yu, *J. Appl. Phys.* **99**, 023703 (2006).
- <sup>25</sup>F. N. Hooge, *Physica B* **311**, 238 (2002).